JOC The Journal of Organic Chemistry

Article

pubs.acs.org/joc

Computational Studies on Pd-Catalyzed Functionalization of C_{sp^2}–H Bonds Using a 1,2,3-Triazole Directing Group: Cyclization versus Substitution

Juan Li,* Lijuan Du, and Honghong Gu

Department of Chemistry, Jinan University, Huangpu Road West 601, Guangzhou, Guangdong 510632, P. R. China

Supporting Information

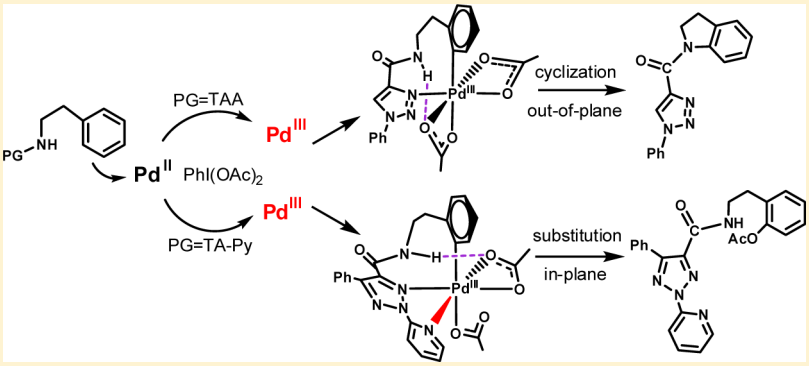

ABSTRACT: The Pd-catalyzed functionalization of C_{sp^2}–H bonds using a 1,2,3-triazole directing group has been investigated by density functional theory calculations at the B3LYP level. The results of these calculations showed that the substitution pathway was kinetically favored over the cyclization pathway for the N2-pyridine-1,2,3-triazole-4-carboxylic acid (TAPy)-directed functionalization of C_{sp^2}–H bonds, while the cyclization pathway was kinetically favored over the substitution pathway for the N1-aryl-1,2,3-triazole-4-carboxylic acid (TAA)-directed C_{sp^2}–H functionalization. The kinetic preference of the TAPy directing group for the substitution reaction can be attributed the reduced level of bond cleavage in the transition structure of the substitution step because the pyridine moiety of the TAPy directing group can act as a ligand for the Pd center.

1. INTRODUCTION

Transition-metal-catalyzed C–H functionalization reactions represent atom economical approaches for the construction of C–C and C–heteroatom bonds.[1] Of the many transition-metal-catalyzed C–H functionalization reactions reported in the literatures, those involving the use of directing groups (DGs) for the selective cleavage of proximal aromatic C–H bonds are particularly important.[2] The use of monodentate DGs in C–H functionalization reactions has been explored extensively.[3] In recent years, there has been growing interest in the use of bidentate DGs in C–H functionalization reactions because they can promote the activation of C–H bonds via the formation of a stoichiometric amount of a stable metallacycle.[4]

Although significant progress has been made toward the development of new methods for the effective functionalization of C_{sp^2}–H bonds using bidentate DGs, the chemoselectivity of these processes remains a significant challenge with competition between the cyclization and substitution reactions. Shi et al.[5] recently reported the development of a Pd(II)-catalyzed C_{sp^2}–H bond activation process that allowed for selective cyclization and substitution reactions through the choice of a suitable directing group. As shown in Scheme 1, the use of an N1-aryl-1,2,3-triazole-4-carboxylic acid (TAA) directing group favored the formation of the cyclization product. In contrast, the use of an N2-pyridine-1,2,3-triazole-4-carboxylic acid (TAPy) directing group favored the formation of the substitution product, even though the cyclization products are usually formed as the major products for most 1,2,3-triazole ligands under identical conditions. Shi et al. proposed the occurrence of Pd(IV) complexes as intermediates in these reactions to explain the differences in the selective cyclization and substitution reactions. According to this explanation, the cyclization reaction would take place through the in-plane mode, while the substitution reaction would occur via an out-of-plane mode for the TAA directing group (Scheme 2). However, the TAPy directing group could force the Pd–C bond into an axial position, which would favor the out-of-plane substitution pathway (Scheme 2).

The occurrence of Pd(IV) intermediates in Pd(II)-catalyzed aromatic C–H functionalization reactions was first proposed in 1971.[6] Canty and co-workers reported the first example of oxidizing a Pd(II) complex to a Pd(IV) species by diphenyliodine(III) triflate.[7] However, the reaction mechanisms involving Pd(III) species have only recently been proposed.[8] With this in mind, there is an important need to determine

Received: September 7, 2015
Published: October 20, 2015

DOI: 10.1021/acs.joc.5b02087
J. Org. Chem. 2015, 80, 10965–10972

Scheme 1. C−H Functionalization with the 1,2,3-Triazole Directing Group

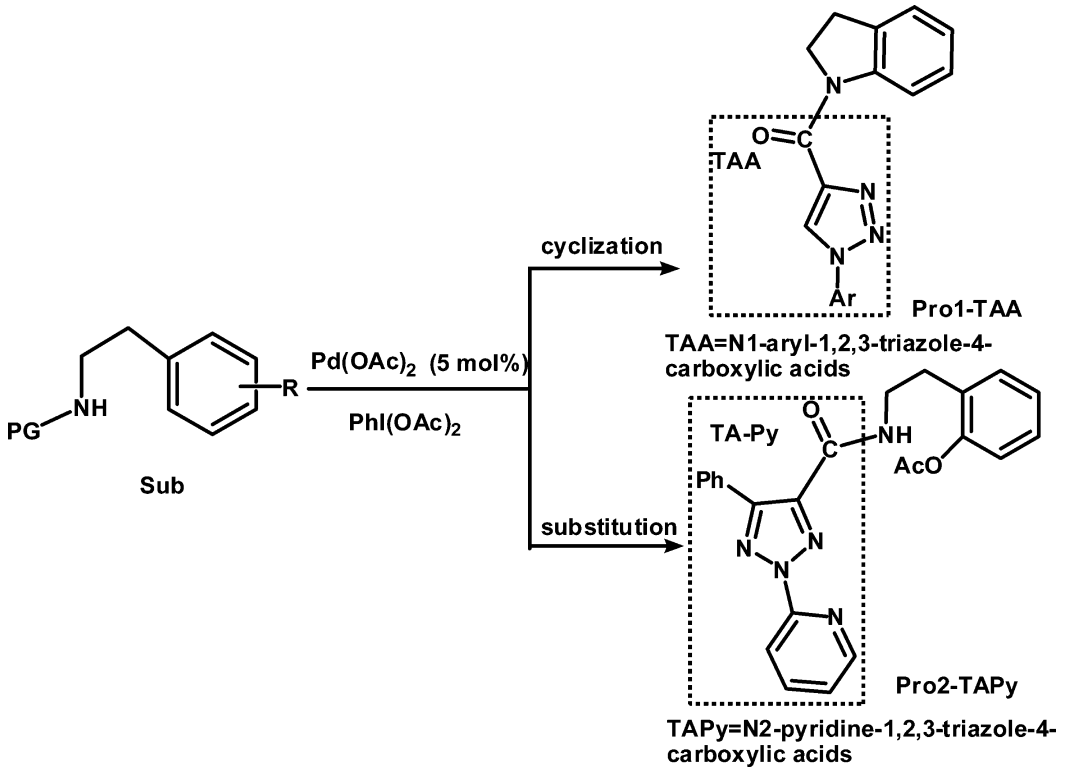

Scheme 2. Nature of the Chemoselectivity Proposed by Shi and Co-workers

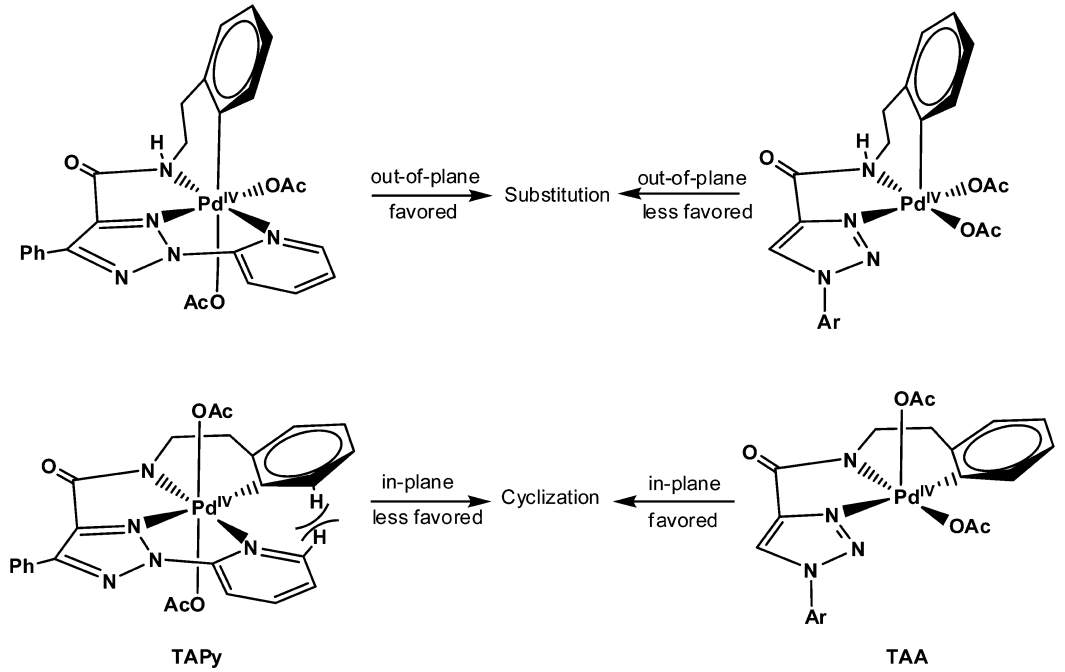

whether a Pd(III) intermediate is involved in Pd(II)-catalyzed C−H functionalization reactions. Despite this need for greater mechanistic understanding, there have been very few computational studies pertaining to the occurrence of Pd(III) intermediate. The groups of Ritter[9] and Yates[10] conducted computational studies which suggested that C−X reductive elimination reactions from binuclear Pd(III) complexes can be facilitated by the synergistic effects of an M−M redox system. Although kinetic studies[11] have been conducted concerning the formation of Pd(IV) intermediates by the oxidation of Pd(II) catalysts with $PhI(OAc)_2$, there have been no studies, to the best of our knowledge, concerning the formation of Pd(III) intermediates in the same way.

In this paper, we report the results of our theoretical calculations toward developing a better understanding of the reaction mechanisms for the chemoselective cyclization and substitution reactions reported by Shi et al. It was envisaged that this study would allow us to determine whether a Pd(III)

DOI: 10.1021/acs.joc.5b02087
J. Org. Chem. 2015, 80, 10965−10972

intermediate was involved in the oxidation and reductive elimination steps of these reactions. We have conducted a theoretical comparison of the reactions involving the two different directing groups, TAA and TAPy, to explain why the TAA directing group undergoes a cyclization reaction, while the TAPy directing group undergoes substitution.

2. COMPUTATIONAL DETAILS

The molecular geometries of the complexes were optimized using DFT calculations at the B3LYP level.[12] Frequency calculations were also performed at the same level of theory to identify all the stationary points as minima (zero imaginary frequencies) or transition states (one imaginary frequency), as well as providing the free energies at 298.15 K. An IRC[13] analysis was performed to confirm that all stationary points were smoothly connected to each other. The Pd and I atoms were described using the LANL2DZ basis set, including a double-valence basis set with the Hay and Wadt effective core potentials.[14] Polarization functions were added for the Pd (ζ_f = 1.472)[15] and I (ζ_d = 0.266)[16] atoms. The 6-31G*[17] basis set was used for all of the other atoms. To test for solvent effects, we also performed single-point energy calculations using the polarizable continuum model (PCM)[18] for all of the gas phase optimized species. The SDD[19] basis sets were used for the Pd and I atoms in the PCM calculations, while the 6-311++G** basis set was used for all of the other atoms. The nonelectrostatic terms (cavity−dispersion−solvent−structure terms) of the solvation energy were calculated using the SMD model[20] to give the final fully corrected free energies (ΔG_{sol}). DCE was used as the solvent, corresponding to the original experimental conditions. We also performed single-point energy calculations using the DFT-D3 empirical dispersion correction by Grimme.[21] All of the calculations described in the current study were performed using the Gaussian 09 software packages.[22]

3. RESULTS AND DISCUSSION

3.1. Cyclization Mechanisms. *3.1.1. C−H Bond-Breaking Step Preceding N−H Bond-Breaking Step (TAA System).* The initial coordination of the substrate to Pd can afford three isomers depending on the different arrangement of the ligand, as shown in Scheme 3. The possible mechanisms for the C−H

Scheme 3. Three Isomers with Different Ligand Arrangements for the TAA System

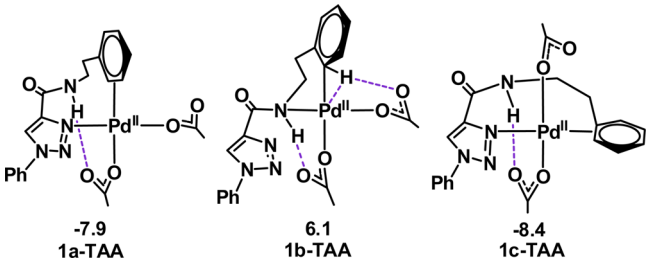

activation for **1a-TAA**, **1b-TAA**, and **1c-TAA** were theoretically investigated: concerted metalation−deprotonation (CMD),[23] oxidative addition,[24] σ-bond metathesis,[25] and anagostic bonding.[26] The CMD mechanisms were found to have the lowest reaction barriers (10.1 and 20.1 kcal/mol) for the arene C−H activation step for **1a-TAA** and **1c-TAA** (Table 1). The anagostic bonding mechanism for **1b-TAA** was found to have the lowest reaction barrier of 12.2 kcal/mol (Table 1). For the discussion below, we have chosen to focus exclusively on the pathway starting from isomer **1a-TAA**, which will be referred to hereafter as the TAA−CH(II)−NH(III) pathway.

Table 1. Solvent- and Dispersion-Corrected Relative Free Energies for Transition States in the CMD, Oxidative Addition, σ-Bond Metathesis, and Anagostic Bonding Mechanisms

	TS1x-TAA-CMD	TS1x-TAA-Oxia	TS1x-TAA-Met	TS1x-TAA-Anag
x = a	2.2	34.6	17.5	not been found
x = b	not been found	31.3	28.2	12.2
x = c	11.7	40.7	25.6	not been found

As shown in Figure 1, **2a-TAA** would release a single molecule of AcOH to form the arylpalladium intermediate **3a-TAA**, which would subsequently undergo an oxidation step. For the oxidation, a molecule of $PhI(OAc)_2$ would approach the Pd center of **3a-TAA** through transition state **TS2a-TAA** to form intermediate **4a-TAA** bearing a Pd−O1 linkage. Compared with isolated $PhI(OAc)_2$, **4a-TAA** had shorter and longer O3−I and O2−I distances, respectively [i.e., both of these values were 2.165 Å for $PhI(OAc)_2$ versus 2.127 and 2.245 Å for **4a-TAA**]. This result indicated that the O2−I bond in **4a-TAA** would be partially broken. The reduction product PhI(OAc) would then be released through transition state **TS3a-TAA** to form the six-coordinate Pd(III) intermediate **5a-TAA** with an energy barrier of 7.3 kcal/mol. The coordination of the amino group and oxygen atom of the OAc ligand to the Pd center would lead to the formation of the six-coordinated intermediate **6a-TAA-Cyc**.

The deprotonation of the amino group would then occur via transition state **TS4a-TAA-Cyc**, followed by the release of a single molecule of AcOH to give the five-coordinated intermediate **8a-TAA-Cyc**. The direct formation of a C−N bond on the Pd(III) intermediate **8a-TAA-Cyc** would occur via a reductive elimination according to the out-of-plane mode to form **9a-TAA-Cyc**. Finally, the Pd−N bond in **9a-TAA-Cyc** would be broken to give the final product **Pro1-TAA**, which would be followed by the regeneration of the catalyst via the oxidization of $PhI(OAc)_2$. The free energy of **TS5a-TAA-Cyc** was determined to be 17.8 kcal/mol higher than that of **8a-TAA-Cyc**. The reductive elimination reaction of **8a-TAA-Cyc** could also occur via transition state **TS5b-TAA-Cyc** according to the in-plane mode (Scheme 4). However, the free energy of **TS5b-TAA-Cyc** was higher than that of **TS5a-TAA-Cyc**. Based on the experimental observations, the reductive elimination would have to take place according to the in-plane mode, which was contrary to the result of our calculation. This difference could be attributed to the trans influence of the phenyl ligand, which could weaken the palladium−ligand interaction at the position trans to the phenyl ligand and destabilize the in-plane transition state. These results therefore suggested that the C−N bond-forming reductive elimination step is rate-determining and that the overall energy barrier for the TAA−CH(II)−NH(III) pathway is 17.9 kcal/mol.

It is noteworthy that **3a-TAA** can also be oxidized by $PhI(OAc)_2$ to afford the Pd(IV) intermediate **5a′-TAA** with the release of PhI, as shown in Figure 2. During the conversion of **4a-TAA** to **TS3a′-TAA**, the O2 and O3 atoms would detach from the I atom with O2···I and O3···I distances of 2.640 and 2.692 Å, and simultaneously the O1 and O4 atoms would approach the Pd atom with Pd−O1 and Pd···O4 distances of 2.112 and 2.406 Å, respectively. The addition of two acetate groups to the Pd center would lead to the formation of the six-coordinate octahedral Pd(IV) complex **5a′-TAA**. This mech-

DOI: 10.1021/acs.joc.5b02087
J. Org. Chem. 2015, 80, 10965−10972

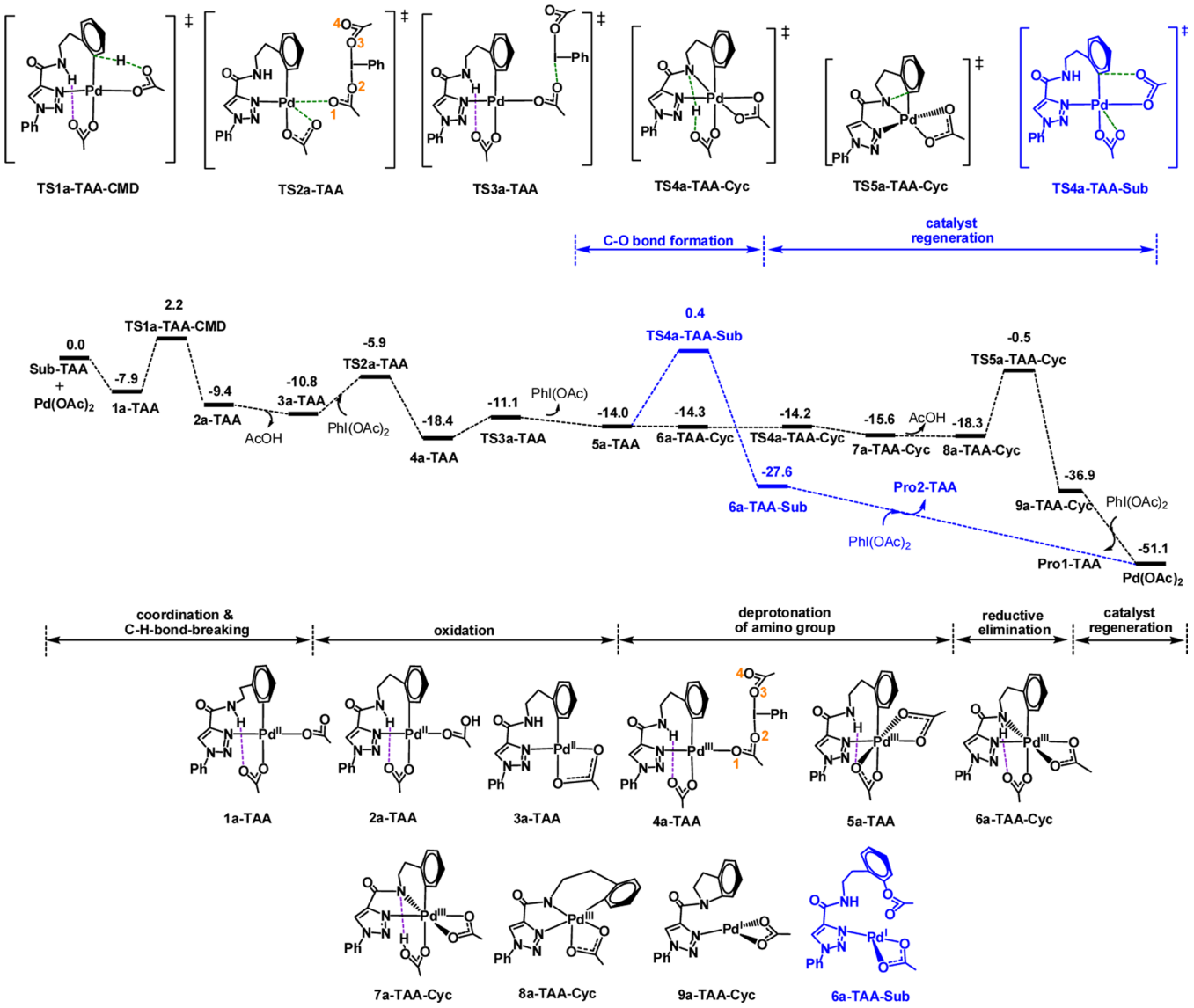

Figure 1. Energy profiles calculated for the TAA-CH(II)-NH(III) and substitution pathways. The solvent- and dispersion-corrected relative free energies are shown in kcal/mol. The atomic numbering scheme is also shown.

Scheme 4. In-Plane Transition States for the C−N Bond-Forming Reductive Elimination Step[a]

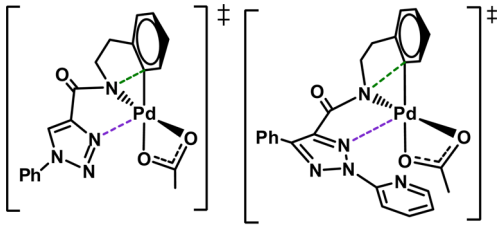

[a]The solvent- and dispersion-corrected relative free energies are shown in kcal/mol.

anistic pathway would require the two added acetate groups to be *cis* orientated with respect to each other, which would be consistent with the experimental observations reported by Fang et al.[10] Although the Pd(IV) intermediate **5a′-TAA** would be much more stable than the Pd(III) intermediate **5a-TAA**, the energy of the corresponding transition state **TS3a′-TAA** (8.0 kcal/mol) would be much higher than that of **TS3a-TAA** (−11.1 kcal/mol), indicating that a pathway involving the Pd(IV) intermediate would be kinetically disfavorable. The kinetic preference for the formation of the Pd(III) intermediate can be attributed to **TS3a′-TAA** being more rigid and formed in much more of a concerted fashion than **TS3a-TAA**.

3.1.2. N−H Bond-Breaking Step Preceding the C−H Bond-Breaking Step (TAA System). This pathway is referred to as the TAA−NH(II)−CH(III) pathway, as shown in Figure 3. The initial deprotonation of the amino group would lead to the formation of intermediate **11-TAA**, which would release a single molecule of AcOH to form **12-TAA**. The subsequent oxidation of **12-TAA** with $PhI(OAc)_2$ would occur via transition states **TS7-TAA** and **TS8-TAA** to afford the Pd(III) intermediate **14-TAA**. The C−H bond-breaking step would then proceed via the CMD mechanism. It is noteworthy, however, that the energy barrier for the C−H bond-breaking transition state **TS9-TAA-CMD** was determined to be

DOI: 10.1021/acs.joc.5b02087
J. Org. Chem. 2015, 80, 10965−10972

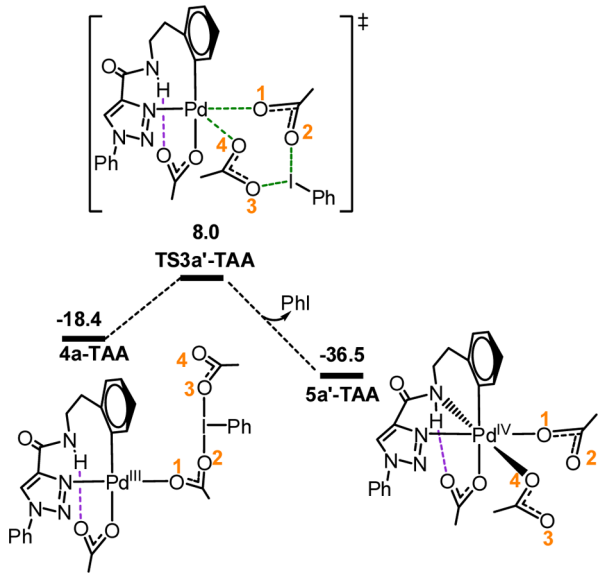

Figure 2. Energy profiles calculated for the oxidation step **4a-TAA** → **5a′-TAA** (Pd^{IV} intermediate) for the TAA system. The solvent- and dispersion-corrected relative free energies are shown in kcal/mol. The atomic numbering scheme is also shown.

relatively higher than that of **13-TAA** (25.4 kcal/mol). The calculated results therefore indicate that the occurrence of a C−H bond-breaking step after the deprotonation of the amino group would be unfavorable, because the Pd(III) center generated by the deprotonation of the amino group would be electron deficient, which would disfavor the subsequent C−H activation process. The occurrence of a C−H activation step prior to the deprotonation of the amino group would prevent this problem.

3.1.3. Cyclization Pathways for the TAPy System. We initially investigated the pathway where the cleavage of the C−H bond preceded the deprotonation of the amino group. The initial coordination of the substrate to Pd could afford several isomers depending on the different arrangement of the ligand, as shown in Scheme 5. The lowest energy barriers for the C−H cleavage steps of **1a-TAPy**, **1b-TAPy**, **1c-TAPy**, **1d-TAPy**, and **1e-TAPy** were determined to be 9.0, 10.1, 20.0, 14.0, and 13.8 kcal/mol, respectively (Table 2). Based on this result, the following discussion is focused entirely on the pathway starting from isomer **1a-TAPy**, which will be referred to hereafter as the TAPy−CH(II)−NH(III) pathway. The overall reaction consisted of four major steps (Figure 4), including (1) **1a-TAPy** → **3a-TAPy** featuring a C−H bond-breaking reaction to give the four-coordinated Pd(II) complex **3a-TAPy** with the release of AcOH; (2) **3a-TAPy** → **5a-TAPy**, which would give the Pd(III) species **5a-TAPy** via a $PhI(OAc)_2$-mediated oxidation; (3) **5a-TAPy** → **8a-TAPy-Cyc**, which would proceed via an N−H bond-cleavage reaction; and (4) **8a-TAPy-Cyc** → **Pro1-TAPy**, which would lead to the formation of the product **Pro1-TAPy** via a C−N bond-forming reductive elimination reaction, which would complete the catalytic cycle and allow for the regeneration of the $Pd(OAc)_2$ catalyst. The overall free energy barrier for the TAPy−CH(II)−NH(III) pathway was calculated to be 18.7 kcal/mol, corresponding to the energy of **TS5a-TAPy-Cyc** relative to **4a-TAPy**. The overall reaction would therefore be an exothermic process with a reaction free energy of −52.3 kcal/mol. Reductive elimination steps occurring via the in-plane mode (Scheme 4) would have to be excluded because the free energy of **TS5b-TAPy-Cyc** was higher than that of **TS5a-TAPy-Cyc**.

In a similar manner to what is shown in Figure 2, intermediate **3a-TAPy** could also be oxidized by $PhI(OAc)_2$ to give a Pd(IV) complex **5a′-TAPy**. However, the energy barrier of the oxidation process for the formation of the Pd(IV)

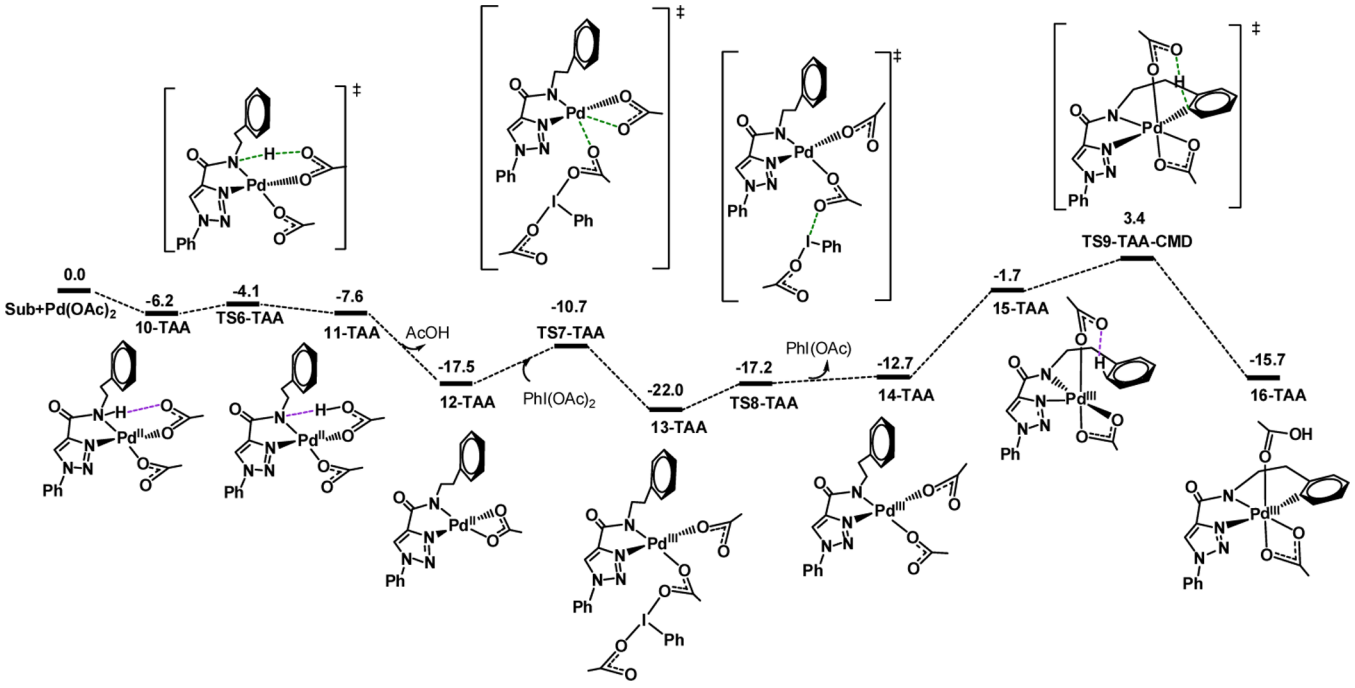

Figure 3. Energy profiles calculated for the deprotonation of the amino group, oxidation and C−H cleavage steps of the TAA-NH(II)−CH(III) pathway. The solvent- and dispersion-corrected relative free energies are shown in kcal/mol.

DOI: 10.1021/acs.joc.5b02087
J. Org. Chem. 2015, 80, 10965−10972

Scheme 5. Several Isomers with Different Ligand Arrangements for the TAPy System

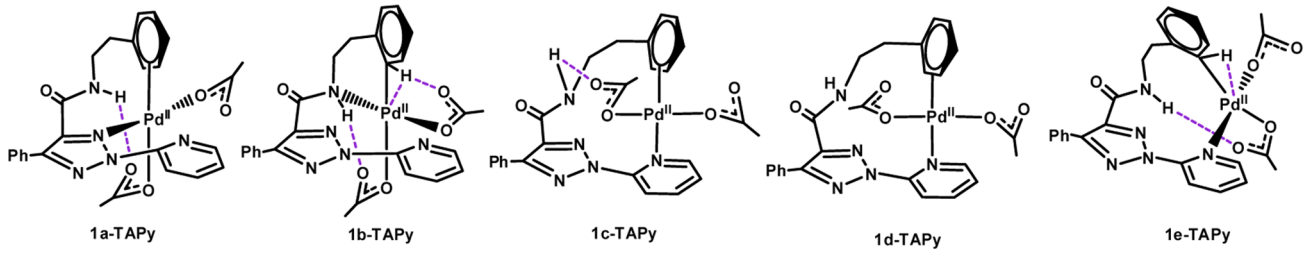

Table 2. Solvent- and Dispersion-Corrected Relative Free Energies for Transition States in the CMD, Oxidative Addition, σ-Bond Metathesis, and Anagostic Bonding Mechanisms

	TS1x-TAPy-CMD	TS1x-TAPy-Oxia	TS1x-TAPy-Met	TS1x-TAPy-Anag
x = a	1.1	29.0	16.8	not been found
x = b	not been found	31.0	25.3	10.1
x = c	6.0	31.4	22.1	not been found
x = d	7.0	32.9	23.7	not been found
x = e	not been found	29.5	not been found	8.3

complex **5a′-TAPy** ($\Delta G^{\#}$ = 29.1 kcal/mol) was determined to be 21.9 kcal/mol higher than that needed to form the Pd(III) complex **5a-TAPy** ($\Delta G^{\#}$ = 7.2 kcal/mol), which indicated that the Pd(IV) intermediate could not have been involved in the Pd(II)-catalyzed selective C_{sp^2}–H activation reaction with the TAPy directing group.

Furthermore, the N–H deprotonation step could only occur if it preceded the C–H bond-breaking step, which is referred to as the TAPy–NH(II)–CH(III) pathway (Figure S1 in the Supporting Information). However, the TAPy–NH(II)–CH-(III) pathway would need to overcome an energy barrier of 25.9 kcal/mol, which is 7.2 kcal/mol higher than that of the TAPy–CH(II)–NH(III) pathway ($\Delta G^{\#}$ = 18.7 kcal/mol).

3.2. Substitution Mechanisms. The C–H bond-breaking and oxidation steps for the substitution pathways are the same as those of the cyclization pathways, leading to the formation of intermediates **5a-TAA** and **5a-TAPy** for the TAA and TAPy systems, respectively. The Ph–OAc coupling reactions of intermediates **5a-TAA** and **5a-TAPy** would occur via the five-membered transition states **TS4a-TAA-Sub** and **TS4a-TAPy-Sub** to form **6a-TAA-Sub** and **6a-TAPy-Sub**, respectively (Figures 1 and 4). The three-membered transition states **TS4a′-TAA-Sub** and **TS4a′-TAPy-Sub** for the formation of the substitution product have also been calculated, as shown in Scheme 6. However, the energies of transition states **TS4a′-TAA-Sub** and **TS4a′-TAPy-Sub** (6.0 and 3.0 kcal/mol) were determined to be much higher than those of **TS4a-TAA-Sub** and **TS4a-TAPy-Sub** (0.4 and −7.5 kcal/mol), respectively. This result indicated that the substitution pathways proceeding via a three-membered transition state were disfavored. This result was therefore consistent with previous calculations for the reductive elimination reactions of C_{sp^2}–acetate bonds using Pd.[27] For the TAPy system, we also considered the possibility that the Ph–OAc coupling step could start from the other isomer **5b-TAPy** (Scheme 7), where the pyridine moiety of the TAPy directing group would act as the ligand. However, the free energy barrier starting from **5b-TAPy** (14.3 kcal/mol) was higher than the energy barrier for starting from **5a-TAPy** (11.2 kcal/mol).

Based on the energy profiles shown in Figure 1, we can conclude that the cyclization pathway involving the TAA directing group was kinetically favored over the substitution pathway. Interestingly, for the TAPy system shown in Figure 4, the substitution pathway was kinetically favored over the cyclization pathway. These results are consistent with the experimental observations,[5] which showed that the TAA directing group mainly gave the cyclization product, while the TAPy directing group mainly gave the substitution product. The reason for the difference between the TAA and TAPy systems is as follows. Notably, the suggestion provided by Shi's group for the selective cyclization and substitution reactions cannot be achieved. We could not locate the tetradentate structures shown in Scheme 2 for the TAPy system because they were too rigid to be obtained. Furthermore, our calculations indicated that the substitution process proceeded according to the in-plane mode, while the cyclization process occurred according to an out-of-plane mode, which are contrary to the suggestions provided by Shi et al. The cyclization processes (**5a-TAA** → **TS4a-TAA-Cyc** versus **5a-TAPy** → **TS4a-TAPy-Cyc**) would be the same because the pyridine moiety of the TAPy directing group would not act as a ligand toward palladium.

For the substitution step **5a-TAA** → **TS4a-TAA-Sub**, the acetate ligand, which would be linked to the Ph group, would need to change from a bidentate to a monodentate ligand. However, the acetate ligand would always exist as a monodentate ligand for **5a-TAPy** → **TS4a-TApy-Sub** because the pyridine moiety of the TAPy directing group can act as a ligand and coordinate to the Pd center. Therefore, the kinetic preference of the substitution process for the TAPy system can be attributed to a reduced level of bond cleavage in the transition structure **TS4a-TApy-Sub** compared with **TS4a-TAA-Sub**.

■ CONCLUSIONS

DFT calculations have been performed to study the $Pd(OAc)_2$-catalyzed activation of C_{sp^2}–H bonds with 1,2,3-triazole directing groups. The competing cyclization and substitution pathways were calculated for the $Pd(OAc)_2$-catalyzed activation of C_{sp^2}–H bonds. The results of these calculations indicated that the cyclization pathways of both the TAA and TAPy systems proceeded as follows: (1) the activation of the arene C–H bonds via a CMD mechanism in which the Pd(II) oxidation state was retained; (2) the oxidation of the arylpalladium(II) intermediate with $PhI(OAc)_2$ to give the corresponding arylpalladium(III) intermediate; (3) the deprotonation of the imino group with Pd(III); and (4) the reductive

DOI: 10.1021/acs.joc.5b02087
J. Org. Chem. 2015, 80, 10965−10972

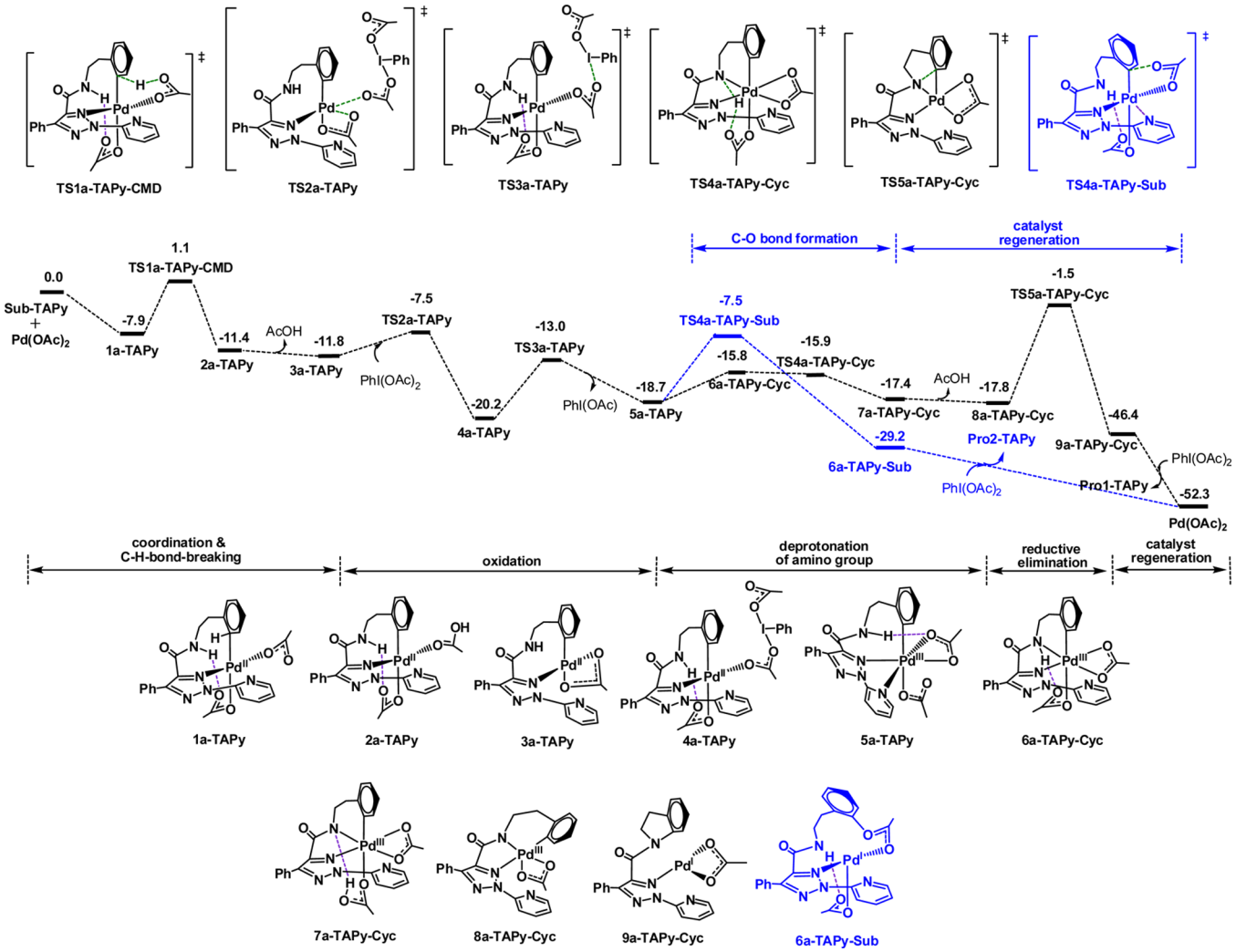

Figure 4. Energy profiles calculated for the TAPy-CH(II)-NH(III) and substitution pathways. The solvent- and dispersion-corrected relative free energies are shown in kcal/mol.

Scheme 6. Three-Membered Transition States for the Ph−OAc Coupling Step

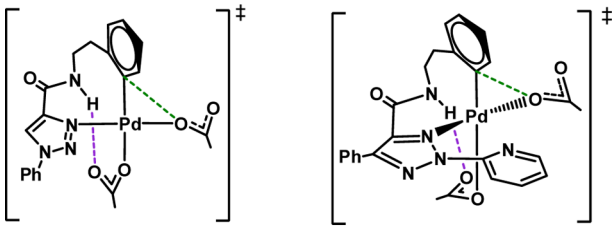

Scheme 7. Ph−OAc Coupling Step Starting from 5b-TAPy[a]

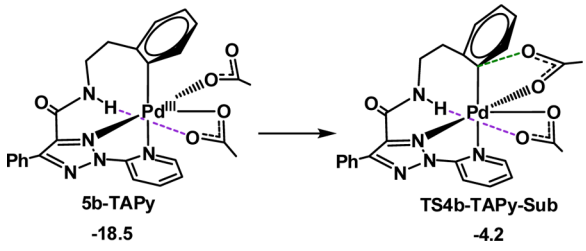

[a]The solvent- and dispersion-corrected relative free energies are shown in kcal/mol.

elimination and C−N bond formation reactions. For the substitution pathway, our calculations supported a three-step-pathway involving (1) C−H activation of the arene C−H bonds with Pd(II) via a CMD process; (2) oxidation of the Pd(II) intermediate; and (3) the coupling of Ph−OAc via a five-membered transition state from Pd(III). For the TAA-directed C_{sp^2}−H activation, the cyclization pathway was kinetically favored over the substitution pathway. In contrast, the TAPy-directed C_{sp^2}−H activation kinetically favored the substitution pathway over the cyclization. The kinetic preference of the TAPy directing group for the substitution process can be attributed to a reduced level of bond cleavage in the transition structure of the substitution step because the pyridine moiety of the TAPy directing group can act as a ligand for the Pd center.

■ ASSOCIATED CONTENT

Supporting Information

The Supporting Information is available free of charge on the ACS Publications website at DOI: 10.1021/acs.joc.5b02087.

DOI: 10.1021/acs.joc.5b02087
J. Org. Chem. 2015, 80, 10965−10972

Complete ref 22, calculated imaginary frequencies of all transition states species, and tables giving Cartesian coordinates and electronic energies for all calculated structures (PDF)

AUTHOR INFORMATION

Corresponding Author

*E-mail: tchjli@jnu.edu.cn.

Notes

The authors declare no competing financial interest.

ACKNOWLEDGMENTS

This work was supported by the National Natural Science Foundation of China (Grant No. 21573095), the Fundamental Research Funds for the Central Universities (Grant No. 21615405), and the high-performance computing platform of Jinan University.

REFERENCES

(1) Recent reviews on selective C−H activation without directing group: (a) Mkhalid, I. A. I.; Barnard, J. H.; Marder, T. B.; Murphy, J. M.; Hartwig, J. F. *Chem. Rev.* **2010**, *110*, 890. (b) Roger, J.; Gottumukkala, A. L.; Doucet, H. *ChemCatChem* **2010**, *2*, 20. (c) Kuhl, N.; Hopkinson, M. N.; Wencel-Delord, J.; Glorius, F. *Angew. Chem., Int. Ed.* **2012**, *51*, 10236. (d) Baillie, R. A.; Legzdins, P. *Acc. Chem. Res.* **2014**, *47*, 330. (e) Li, B.; Dixneuf, P. H. *Chem. Soc. Rev.* **2013**, *42*, 5744. (f) Sambiagio, C.; Marsden, S. P.; Blacker, A. J.; McGowan, P. C. *Chem. Soc. Rev.* **2014**, *43*, 3525. (g) Yuan, K.; Soulé, J.-F.; Doucet, H. *ACS Catal.* **2015**, *5*, 978.

(2) Recent reviews on directed C−H activation: (a) Huang, H.; Ji, X.; Wu, W.; Jiang, H. *Chem. Soc. Rev.* **2015**, *44*, 1155. (b) Yamaguchi, J.; Yamaguchi, A. D.; Itami, K. *Angew. Chem., Int. Ed.* **2012**, *51*, 8960. (c) Rouquet, G.; Chatani, N. *Angew. Chem., Int. Ed.* **2013**, *52*, 11726. (d) Wencel-Delord, J.; Glorius, F. *Nat. Chem.* **2013**, *5*, 369. (e) De Sarkar, S.; Liu, W.; Kozhushkov, S. I.; Ackermann, L. *Adv. Synth. Catal.* **2014**, *356*, 1461. (f) Gao, K.; Yoshikai, N. *Acc. Chem. Res.* **2014**, *47*, 1208. (g) Miura, M.; Satoh, T.; Hirano, K. *Bull. Chem. Soc. Jpn.* **2014**, *87*, 751. (h) Ros, A.; Fernández, R.; Lassaletta, J. M. *Chem. Soc. Rev.* **2014**, *43*, 3229. (i) Song, G.; Li, X. *Acc. Chem. Res.* **2015**, *48*, 1007. (j) Yang, L.; Huang, H. *Chem. Rev.* **2015**, *115*, 3468.

(3) Selected examples: (a) Ackermann, L. *Chem. Rev.* **2011**, *111*, 1315. (b) Yeung, C. S.; Dong, V. M. *Chem. Rev.* **2011**, *111*, 1215. (c) Neufeldt, S. R.; Sanford, M. S. *Acc. Chem. Res.* **2012**, *45*, 936. (d) Engle, K. M.; Mei, T.-S.; Wasa, M.; Yu, J.-Q. *Acc. Chem. Res.* **2012**, *45*, 788. (e) Colby, D. A.; Tsai, A. S.; Bergman, R. G.; Ellman, J. A. *Acc. Chem. Res.* **2012**, *45*, 814. (f) Arockiam, P. B.; Bruneau, C.; Dixneuf, P. H. *Chem. Rev.* **2012**, *112*, 5879. (g) Zhou, B.; Chen, H.; Wang, C. *J. Am. Chem. Soc.* **2013**, *135*, 1264.

(4) Selected examples for C(sp^2)−H activation: (a) Kanyiva, K. S.; Kuninobu, Y.; Kanai, M. *Org. Lett.* **2014**, *16*, 1968. (b) Al Mamari, H. H.; Diers, E.; Ackermann, L. *Chem. - Eur. J.* **2014**, *20*, 9739. (c) Shang, M.; Sun, S.-Z.; Dai, H.-X.; Yu, J.-Q. *J. Am. Chem. Soc.* **2014**, *136*, 3354. (d) Ye, X. H.; Shi, X. D. *Org. Lett.* **2014**, *16*, 4448. (e) Deb, A.; Bag, S.; Kancherla, R.; Maiti, D. *J. Am. Chem. Soc.* **2014**, *136*, 13602. (f) Gu, Q.; Al Mamari, H. H.; Graczyk, K.; Diers, E.; Ackermann, L. *Angew. Chem., Int. Ed.* **2014**, *53*, 3868. (g) Chen, K.; Li, Z.-W.; Shen, P.-X.; Zhao, H.-W.; Shi, Z.-J. *Chem. - Eur. J.* **2015**, *21*, 7389. (h) Wang, C.; Chen, C.; Zhang, J.; Han, J.; Wang, Q.; Guo, K.; Liu, P.; Guan, M.; Yao, Y.; Zhao, Y. *Angew. Chem., Int. Ed.* **2014**, *53*, 9884. (i) Daugulis, O.; Roane, J.; Tran, L. D. *Acc. Chem. Res.* **2015**, *48*, 1053. (j) Zhang, D.; Gao, F.; Nian, Y.; Zhou, Y.; Jiang, H.; Liu, H. *Chem. Commun.* **2015**, *51*, 7509. (k) Tang, H.; Zhou, B.; Huang, X.-R.; Wang, C.; Yao, J.; Chen, H. *ACS Catal.* **2014**, *4*, 649. (l) Han, J.; Liu, P.; Wang, C.; Wang, Q.; Zhang, J.; Zhao, Y.; Shi, D.; Huang, Z.; Zhao, Y. *Org. Lett.* **2014**, *16*, 5682.

(5) Ye, X.; He, Z.; Ahmed, T.; Weise, K.; Akhmedov, N. G.; Petersen, J. L.; Shi, X. *Chem. Sci.* **2013**, *4*, 3712.

(6) Henry, P. M. *J. Org. Chem.* **1971**, *36*, 1886.

(7) Canty, A. J.; Patel, J.; Rodemann, T.; Ryan, J. H.; Skelton, B. W.; White, A. H. *Organometallics* **2004**, *23*, 3466.

(8) (a) Lanci, M. P.; Remy, M. S.; Kaminsky, W.; Mayer, J. M.; Sanford, M. S. *J. Am. Chem. Soc.* **2009**, *131*, 15618. (b) Powers, D. C.; Ritter, T. *Nat. Chem.* **2009**, *1*, 302.

(9) Powers, D. C.; Benitez, D.; Tkatchouk, E.; Goddard, W. A., III; Ritter, T. *J. Am. Chem. Soc.* **2010**, *132*, 14092.

(10) Ariafard, A.; Hyland, C. J. T.; Canty, A. J.; Sharma, M.; Yates, B. F. *Inorg. Chem.* **2011**, *50*, 6449.

(11) Lian, B.; Zhang, L.; Chass, G. A.; Fang, D.-C. *J. Org. Chem.* **2013**, *78*, 8376.

(12) (a) Becke, A. D. *J. Chem. Phys.* **1993**, *98*, 5648. (b) Lee, C.; Yang, W.; Parr, R. G. *Phys. Rev. B: Condens. Matter Mater. Phys.* **1988**, *37*, 785. (c) Stephens, P. J.; Devlin, F. J.; Chabalowski, C. F.; Frisch, M. J. *J. Phys. Chem.* **1994**, *98*, 11623.

(13) (a) Fukui, K. *J. Phys. Chem.* **1970**, *74*, 4161. (b) Fukui, K. *Acc. Chem. Res.* **1981**, *14*, 363.

(14) (a) Hay, P. J.; Wadt, W. R. *J. Chem. Phys.* **1985**, *82*, 299. (b) Wadt, W. R.; Hay, P. J. *J. Chem. Phys.* **1985**, *82*, 284.

(15) Ehlers, A. W.; Böhme, M.; Dapprich, S.; Gobbi, A.; Höllwarth, A.; Jonas, V.; Köhler, K. F.; Stegmann, R.; Veldkamp, A.; Frenking, G. *Chem. Phys. Lett.* **1993**, *208*, 111.

(16) Huzinaga, S. *Gaussian Basis Sets for Molecular Calculations*; Elsevier Science Pub. Co.: Amsterdam, 1984.

(17) Hariharan, P. C.; Pople, J. A. *Theor. Chim. Acta* **1973**, *28*, 213.

(18) (a) Barone, V.; Cossi, M. *J. Phys. Chem. A* **1998**, *102*, 1995. (b) Cossi, M.; Rega, N.; Scalmani, G.; Barone, V. *J. Comput. Chem.* **2003**, *24*, 669. (c) Tomasi, J.; Mennucci, B.; Cammi, R. *Chem. Rev.* **2005**, *105*, 2999.

(19) (a) Fuentealba, P.; Preuss, H.; Stoll, H.; Von Szentpaly, L. *Chem. Phys. Lett.* **1982**, *89*, 418. (b) von Szentpaly, L.; Fuentealba, P.; Preuss, H.; Stoll, H. *Chem. Phys. Lett.* **1982**, *93*, 555. (c) Fuentealba, P.; Stoll, H.; Szentpaly, L. V.; Schwerdtfeger, P.; Preuss, H. *J. Phys. B: At. Mol. Phys.* **1983**, *16*, L323.

(20) Marenich, A. V.; Cramer, C. J.; Truhlar, D. G. *J. Phys. Chem. B* **2009**, *113*, 6378.

(21) Grimme, S.; Antony, J.; Ehrlich, S.; Krieg, H. *J. Chem. Phys.* **2010**, *132*, 154104.

(22) Frisch, M. J. *Gaussian 09*, revision C.01; Gaussian, Inc: Wallingford, CT, 2010. [Full reference given in Supporting Information.]

(23) Our recent theoretical study for the Cu- and Pd-catalyzed intramolecular C−H activation of *N*-arylamidines: Li, J.; Gu, H. H.; Wu, C. H.; Du, L. J. *Dalton Trans.* **2014**, *43*, 16769.

(24) (a) Mota, A. J.; Dedieu, A.; Bour, C.; Suffert, J. *J. Am. Chem. Soc.* **2005**, *127*, 7171. (b) Campo, M. A.; Huang, Q.; Yao, T.; Tian, Q.; Larock, R. C. *J. Am. Chem. Soc.* **2003**, *125*, 11506. (c) Capito, E.; Brown, J. M.; Ricci, A. *Chem. Commun.* **2005**, 1854. (d) Canty, A. J.; van Koten, G. *Acc. Chem. Res.* **1995**, *28*, 406.

(25) (a) Zhang, S.; Shi, L.; Ding, Y. *J. Am. Chem. Soc.* **2011**, *133*, 20218. (b) Gómez, M.; Granell, J.; Martinez, M. *Organometallics* **1997**, *16*, 2539. (c) Gómez, M.; Granell, J.; Martinez, M. *J. Chem. Soc., Dalton Trans.* **1998**, 37.

(26) (a) Babić, D.; Ćurić, M.; Smith, D. M. *J. Organomet. Chem.* **2011**, *696*, 661. (b) Rousseaux, S.; Davi, M.; Sofack-Kreutzer, J.; Pierre, C.; Kefalidis, C. E.; Clot, E.; Fagnou, K.; Baudoin, O. *J. Am. Chem. Soc.* **2010**, *132*, 10706. (c) Chaumontet, M.; Piccardi, R.; Audic, N.; Hitce, J.; Peglion, J.-L.; Clot, E.; Baudoin, O. *J. Am. Chem. Soc.* **2008**, *130*, 15157. (d) Davies, D. L.; Donald, S. M. A.; Macgregor, S. A. *J. Am. Chem. Soc.* **2005**, *127*, 13754. (e) Wu, J.-Q.; Qiu, Z.-P.; Zhang, S.-S.; Liu, J.-G.; Lao, Y.-X.; Gu, L.-Q.; Huang, Z.-S.; Li, J.; Wang, H. *Chem. Commun.* **2015**, *51*, 77.

(27) Gary, J. B.; Sanford, M. S. *Organometallics* **2011**, *30*, 6143.

DOI: 10.1021/acs.joc.5b02087
J. Org. Chem. 2015, 80, 10965−10972